Wave loading on ships and platforms at a small forward speed

by John Grue and Enok Palm

Department of Mechanics
University of Oslo, Norway

1 Abstract

Forces on marine structures oscillating in incoming waves with a small forward speed are studied. Coupling between the oscillatory wave field and the steady flow around the body is accounted for. Friction and separation effects are disregarded, and the fluid flow is modelled by potential theory. The boundary value problem for the velocity potential is transformed to an integral equation by Green's theorem, using a Green function satisfying the linear free surface condition with small forward speed. This integral equation contains unknowns on the wetted body surface and on a region of the free surface close to the body. Local, small forward speed expansions for the potential and the Green function are introduced in the vicinity of the body, giving two sets of integral equations for the unkown zero speed and the small forward speed potentials. These integral equations contain unknowns on the wetted body surface only. The right hand side of the small forward speed integral equation involves a fast decaying integral over the free surface. There is no water line integral in the integral equations. The method is applicable to bodies of arbitrary shape. The diagonal added mass and damping coefficients are found to be functions of the forward speed only through the encounter frequency. The linear exciting forces are found by generalized Haskind relations. The mean second order horizontal drift forces and the mean second order yaw moment are discussed, and numerical examples are presented for a ship and a platform. The mean drift forces are usually increased by a small forward speed against the incoming wave direction. For complex body geometries the wave drift damping may, however, in narrow wave number regions, become negative. Numerical examples show that the mean drift force and the mean yaw moment may be changed by 100% even for a small forward speed.

2 Introduction

The combined interaction between waves and a floating body with a small forward speed is an important issue within offshore technology. The major reason for this is that a forward speed of the body introduces significant changes in the waves which are scattered by the body, even when the forward speed is very small. The wave drift force acting on the floating body, which is proportional to the square of the scattered wave amplitudes, is consequently strongly influenced by a small forward speed. The effect of a small forward speed on the mean drift forces may easily be understood if we consider a freely floating body which is drifting with a constant average speed in the direction of the incoming waves due to the action of the waves alone. According to Newtons's second law there must then be a vanishing mean force on the body since the speed is constant. Assuming that the wave drift forces are the dominating forces which is acting on the body, we may conclude that the forward speed has introduced a change in the mean drift force which is of equal magnitude as the mean drift force at zero forward speed. In other words, a small forward speed may change the mean drift force of the order of 100%.

This strong effect of a small forward speed has prooved to be an important damping mechanism of induced resonant slow drift motions of floating and moored ships and oil platforms, where damping forces due to viscous effects and wave radiation may be small. This damping mechanism is called wave drift damping. By a Taylor expansion of the wave drift force in the forward speed, keeping the zero forward speed term and the linear term in the forward speed, and neglecting higher order terms, the wave drift damping acts as an ordinary linear damping force. The wave drift damping is positive in most cases. However, in some cases the wave drift damping becomes negative and may then destabilize the slow drift motions of the body. Negative wave drift damping may occur in narrow wave number regions for complex body geometries were resonance between the different components of the body may occur. This will be true for a TLP-platform.

The practical effect of the wave drift damping and the computational aspects of it has been studied by Wichers and Sluijs (1979) in connection with free decaying model tests, and by Wichers and Huismans (1984), Zhao, Faltinsen, Krokstad and Aanesland (1988), Zhao and Faltinsen (1989) and Wu and Eatock-Taylor (1990).

Here we will present a summary of a theoretical approach developed by Nossen, Grue and Palm (1991) and Grue and Palm (1991) on the combined effect between waves and a three-dimensional body of arbitrary shape and with a small forward speed. Basic assumptions are that viscous forces may be neglected, the flow is irrotational and the fluid is compressible, so potential theory can be used. The boundary conditions are linearized with respect to the amplitude of the incoming waves and the forward velocity. The boundary value problem is decomposed into a steady part, accounting for the steady flow around the body, and an oscillatory part due to the incoming and scattered waves by the body. The free surface boundary condition for the steady velocity potential is approximated by the rigid wall boundary condition since we are neglecting quadratic terms in the forward speed. For the oscillatory part of the problem we apply Green's theorem to obtain an integral equation for the oscillatory potential, which involves unknowns at the wetted surface of the body and at the free surface. The free surface integral decays, however, rapidly. There are no waterline integral in the integral equations.

In the vicinity of the body we expand the Green function and the oscillatory potential in asymptotic series after the forward speed, keeping linear terms. These expansions reduce the integral equation to two sets of integral equations with unknowns at the wetted body surface only. Furthermore, the small forward speed Green function may be obtained by the zero speed Green function for which efficient subroutines exist.

We shortly summarize the results conserning the linear wave forces. It was shown by Wu and Eatock-Taylor (1990) and by Nossen, Grue and Palm (1991) that the well known Timman-Newman relations are valid for bodies of arbitrary shape also when the exact steady potential is accounted for. Nossen, Grue and Palm also derived a generalized Haskind relation which gives the exciting forces directly by the far-field amplitudes of the radiation potentials. The mean horizontal drift forces and the mean yaw moment are obtained by the momentum theorem and by using the far-field values of the velocity potentials. Numerical examples show that the effect of a forward speed on the linear forces is moderate. A small forward speed gives, however, pronounced changes, of the order of 100% , of the quadratic mean drift forces. Numerical examples are presented for a ship and an oil platform. For slow surge motions of the ship, with speed up to $1 - 2ms^{-1}$, we conclude that the wave drift damping is a much stronger damping force than the friction drag. We also find that the wave drift damping is comparable with the drag forces on the platform due to separated flow.

3 The boundary value problem

Let us consider the problem in the frame of reference translating with the steady forward speed of the body, and let us introduce a coordinate system $O - xyz$ with the x- and y-axes in the mean free surface and the z-axis vertical upwards. Let furthermore the ambient horizontal current, with constant speed U, be directed along the negative x-axis. The fluid is assumed to be homogenous and incompressible, and the motion irrotational. The velocity is then given by the gradient of a velocity potential Φ, i.e. $\boldsymbol{v} = \nabla\Phi$, which satisfies the Laplace equation. Φ is composed by a steady potential $U\chi_s$ due to the current and the stationary flow around the body, and a time dependent part $\Re\phi e^{i\sigma t}$ due to incoming and scattered time harmonic waves, as well as waves generated by the oscillatory motions of the body:

$$\Phi(\boldsymbol{x}, t) = U\chi_s(\boldsymbol{x}) + \Re\phi(\boldsymbol{x})e^{i\sigma t} \tag{1}$$

where t denotes time and σ the frequency of encounter.

The potentials χ_s and ϕ are subject to boundary conditions on the free surface, the mean position of the body and far away from the body. The boundary value problem for χ_s is, to first order in U, given by

$$\nabla^2\chi_s = 0 \qquad \text{in the fluid} \tag{2}$$

subject to

$$\frac{\partial\chi_s}{\partial z} = 0 \qquad \text{at } z = 0 \tag{3}$$

$$\frac{\partial\chi_s}{\partial n} = 0 \qquad \text{on } S_B \tag{4}$$

$$\nabla\chi_s = -U\boldsymbol{i} \qquad |\boldsymbol{x}| \to \infty \tag{5}$$

where $\partial/\partial n$ denotes differentiation along the unit normal $\boldsymbol{n}$ of the body surface, pointing out of the fluid, $\boldsymbol{i}$ denotes the unit vector along the x-axis and S_B denotes the mean position of the body. Decomposing χ_s into

$$\chi_s = \chi - x \tag{6}$$

the steady problem is solved by applying a source distribution over the body surface for the potential χ. The potential ϕ may be decomposed by

$$\phi(\boldsymbol{x}) = A\frac{ig}{\omega}(\phi_0(\boldsymbol{x}) + \phi_7(\boldsymbol{x})) + i\sigma\sum_{j=1}^{6}\xi_j\phi_j(\boldsymbol{x}) \tag{7}$$

Here A denotes the amplitude of the incoming waves, ω the orbital frequency of the incoming waves, and g the acceleration due to gravity. ϕ_0 and ϕ_7 denote the incoming wave and scattering potentials, respectively, ξ_j denotes the amplitude of the body motion in the jth mode (surge, sway, heave, roll, pitch and yaw, respectively), and ϕ_j is the corresponding radiation potential for unit amplitude of motion. The incoming wave potential for incident wave angle β reads

$$\phi_0 = e^{Kz - iK(x\cos\beta + y\sin\beta)} \tag{8}$$

where K is the wave number of the incoming waves related to the orbital frequency by the dispersion relation for gravity waves in water of infinite depth

$$K = \omega^2/g \tag{9}$$

The frequency of encounter σ is related to ω and U by

$$\sigma = \omega - U\frac{\omega^2}{g}\cos\beta \tag{10}$$

The case $\beta = 0$ corresponds to following waves, while $\beta = \pi$ corresponds to head waves.

Let us then consider the boundary value problems for $\phi_j, j = 1, ...7$. According to the previous assumptions, each ϕ_j satisfies the Laplace equation. At the free surface, the radiation potentials and the diffraction potential $\phi_D = \phi_0 + \phi_7$ satisfy

$$-\nu\phi + 2i\tau\nabla_1\phi\cdot\nabla_1\chi_s + i\tau\phi\nabla_1^2\chi_s + \frac{\partial\phi}{\partial z} = 0 \text{ at } z = 0 \tag{11}$$

where ∇_1 denotes the horizontal gradient, $\nu = \sigma^2/g$ and $\tau = U\sigma/g$. Far away from the body, $\chi_s \to -x$, and the free surface boundary condition simplifies to

$$-\nu\phi_j - 2i\tau\frac{\partial\phi_j}{\partial x} + \frac{\partial\phi_j}{\partial z} = 0 \text{ at } z = 0 \tag{12}$$

The body boundary conditions for the unknown potentials are given by (Newman 1978)

$$\frac{\partial\phi_j}{\partial n} = \begin{cases} n_j + \frac{U}{i\sigma}m_j, & j = 1, \ldots, 6 \\ -\frac{\partial\phi_0}{\partial n}, & j = 7 \end{cases} \tag{13}$$

where $(n_1, n_2, n_3) = \boldsymbol{n}$, $(n_4, n_5, n_6) = \boldsymbol{x} \times \boldsymbol{n}$,

$$(m_1, m_2, m_3) = -\boldsymbol{n}\cdot\nabla(\nabla\chi_s) \tag{14}$$

$$(m_4, m_5, m_6) = -\boldsymbol{n}\cdot\nabla(\boldsymbol{x}\times\nabla\chi_s) \tag{15}$$

Far away from the body, the radiation conditions state that the radiation potentials and the scattering potential behave as outgoing waves:

$$\phi_j = R^{-1/2}H_j(\theta)e^{k_1(\theta)(z - iR\sqrt{1-4\tau^2\sin^2\theta})} + O(\frac{1}{R}) \qquad \text{as } R - \infty \tag{16}$$

(see Section 4), where $x = R\cos\theta, y = R\sin\theta$. The angle dependent wave number $k_1(\theta)$ is given in the next section by eq. (24). $H_j(\theta)$ denotes the amplitude distribution of the jth radiation or the scattering potential.

4 The Green function

The radiation and diffraction problems with the boundary condition (11) at the free surface and the boundary conditions (13) on the wetted body surface will be solved by applying Green's second identity to the entire fluid domain. As Green function we apply a pulsating source translating with small forward speed and satisfying the free surface condition (12). This function is given by

$$G(\boldsymbol{x},\boldsymbol{\xi}) = \frac{1}{r} - \frac{1}{r'} + \Psi(\boldsymbol{x},\boldsymbol{\xi}) \tag{17}$$

where $\boldsymbol{x} = (x, y, z)$, $\boldsymbol{\xi} = (\xi, \eta, \zeta)$, $r = |\boldsymbol{x} - \boldsymbol{\xi}|$ and $r' = |\boldsymbol{x} - (\xi, \eta, -\zeta)|$ and the wave part of the source potential given by

$$\Psi(\boldsymbol{x},\boldsymbol{\xi}) = \frac{1}{\pi} \int_0^{2\pi} \int_0^{\infty} \frac{E(\alpha, k) dk d\alpha}{(k - \kappa_1)(1 + 2\tau \cos \alpha)} \tag{18}$$

where

$$E(\alpha, k) = k \exp\left[k(z + \zeta) + ik\left((x - \xi)\cos\alpha + (y - \eta)\sin\alpha\right)\right] \tag{19}$$

The path of integration is above the pole $k = \kappa_1$ given by

$$\kappa_1(\alpha) = \frac{\nu}{1 + 2\tau \cos \alpha} \tag{20}$$

The far-field behaviour of G, which will be used later, is obtained by applying contour integration and the method of stationary phase, giving

$$G(R, \theta, z; \xi, \eta, \zeta) = R^{-1/2} h(\xi, \theta) e^{k_1(\theta)(z + iR\cos(\alpha_0 - \theta))} + \mathcal{O}\left(\frac{1}{R}\right) \tag{21}$$

where the stationary phase angle $\alpha_0(\theta)$ is given by

$$\sin(\alpha_0 - \theta) = 2\tau \sin\theta, \;\; \cos(\alpha_0 - \theta) < 0 \tag{22}$$

Thus, we have

$$\cos(\alpha_0 - \theta) = -\sqrt{1 - 4\tau^2 \sin^2\theta} \tag{23}$$

Furthermore, the wave number of the outgoing waves is given by

$$k_1(\theta) = \frac{\nu}{1 + 2\tau \cos \alpha_0(\theta)} \tag{24}$$

Hence,

$$G(R, \theta, z; \xi, \eta, \zeta) = R^{-1/2} h(\xi, \theta) e^{k_1(\theta)(z - iR\sqrt{1 - 4\tau^2 \sin^2\theta})} + \mathcal{O}\left(\frac{1}{R}\right) \tag{25}$$

where

$$h(\xi, \theta) = \sqrt{\frac{8\pi}{\nu}} k_1(\theta) e^{k_1(\theta)[\zeta + i\xi(\cos\theta + 2\tau\sin^2\theta) + i\eta(\sin\theta - 2\tau\cos\theta\sin\theta)] - i\pi/4} + \mathcal{O}(\tau^2) \tag{26}$$

5 Solution of the boundary value problems

The boundary value problems are solved by applying Green's theorem to G and $\phi_D = \phi_0 + \phi_7$ in the diffraction problem, and G and $\phi_j, j = 1, ...6$ in the radiation problems. Let S_F denote the free surface and S_∞ denote a vertical cylinder enclosing the fluid at infinity. Considering the diffraction problem first, Green's theorem gives

$$\iint_{S_B} \phi_D \frac{\partial G}{\partial n} dS + \iint_{S_F+S_\infty} \left(\phi_D \frac{\partial G}{\partial n} - G\frac{\partial \phi_D}{\partial n}\right) dS = \left\{ \begin{array}{l} -4\pi\phi_D(\boldsymbol{x}) \\ -2\pi\phi_D(\boldsymbol{x}) \end{array} \right. \tag{27}$$

where the first case applies to $\boldsymbol{x}$ in the fluid domain and the second to $\boldsymbol{x}$ on the wetted body surface. On the free surface ϕ_D satisfies the variable-coefficient condition (11), while the Green function satisfies (12). It was shown in Nossen, Grue and Palm (1991) that (27), omitting terms of order τ^2 and smaller, reduces to

$$\begin{array}{r} \displaystyle\iint_{S_B} \phi_D \frac{\partial G}{\partial n} dS \\ \displaystyle -2i\tau \iint_{S_F} \phi_D(\nabla_1 G \cdot \nabla_1 \chi + \frac{1}{2} G \nabla_1^2 \chi) dS - 4\pi\phi_0 = \left\{ \begin{array}{l} -4\pi\phi_D(\boldsymbol{x}) \\ -2\pi\phi_D(\boldsymbol{x}) \end{array} \right. \end{array} \tag{28}$$

We note that (28) include integrals over the body and the free surface.

Using the boundary condition (13) on the body, the corresponding result for the radiation problems can be shown to be

$$\begin{array}{r} \displaystyle\iint_{S_B} \left(\phi_j \frac{\partial G}{\partial n} - G(n_j + \frac{U}{i\sigma} m_j)\right) dS \\ \displaystyle -2i\tau \iint_{S_F} \phi_j(\nabla_1 G \cdot \nabla_1 \chi + \frac{1}{2} G \nabla_1^2 \chi) dS = \left\{ \begin{array}{l} -4\pi\phi_j(\boldsymbol{x}) \\ -2\pi\phi_j(\boldsymbol{x}) \end{array} \right. \end{array} \tag{29}$$

for $j = 1, \ldots, 6$.

We note that the equations (28) - (29) contain no water line integral. In the full linear three-dimensional problem, the steady disturbance χ is usually neglected, leading to integral equations containing a waterline integral. In our case, this integral vanishes because the steady potential $U\chi_s$ satisfies the correct boundary condition (4) on the body surface. Instead of the waterline integral, our equations contain an integral over the free surface. This integral, however, decays very rapidly with increasing distance from the body, since it contains the spatial derivatives of the steady disturbance χ, and χ behaves as a dipole far from the body. Therefore we may always truncate the free surface at a quite short distance from the body.

The integral equations (28) and (29) for the unknown potentials ϕ_j and ϕ_D on the body may be simplified by assuming that the reduced frequency $\tau \ll 1$. Expanding ϕ and G in asymptotic series of τ, and keeping only linear terms, we have

$$\phi = \phi^0 + \tau\phi^1 \tag{30}$$

$$G = G^0 + \tau G^1 \tag{31}$$

where

$$G^0 = \frac{1}{r} - \frac{1}{r'} + 2 \int_0^\infty \frac{k e^{k(z+\zeta)}}{k - \nu} J_0(kR') dk \tag{32}$$

Here, $R' = \sqrt{(x-\xi)^2 + (y-\eta)^2}$, J_0 is the Bessel function of the first kind and zero order and $\nu = \sigma^2/g$. Following Huismans and Hermans (1985), the first-order correction term can be written as

$$G^1 = -4i\frac{x-\xi}{R'} \oint_0^\infty \frac{k^2 e^{k(z+\zeta)}}{(k-\nu)^2} J_1(kR')dk \tag{33}$$

where J_1 is the Bessel function of the first kind and first order. It is seen that G^1 may be written very shortly in the form

$$G^1 = 2i\frac{\partial^2 G^0}{\partial\nu\partial x} \tag{34}$$

Thus, the Green function for small forward speed can be expressed by means of the real and imaginary parts of the zero-speed Green function and its derivatives.

The integrals of the m-terms, appearing in the integral equations for the radiation potentials, are on an undesirable form. These integrals may be rewritten by using Tuck's theorem (Ogilvie and Tuck 1969), giving

$$\iint_{S_B} \nabla\chi_s \cdot \nabla G n_j dS = -\iint_{S_B} G m_j dS - \int_{C_B} G\frac{\partial \chi_s}{\partial z} n_j ds \tag{35}$$

provided that the wetted surface S_B is smooth and that it is wall-sided at the free surface. In our case, the waterline contribution in Tuck's theorem vanishes due to the rigid wall condition (3). It should be noted here that Tuck's theorem is, strictly speaking, not valid for G which is not a continous function on the body. This is circumvented by putting x in the fluid and let it approach the body boundary. Since the right hand side of (35) exists in the limit, also the left hand side must exist in the limit. It follows that the left hand side of (35) is a principal value integral since $n \cdot \nabla\chi_s = 0$ on the body boundary.

Thus, introducing the asymptotic expansions into (28) and (29), applying Tuck's theorem and collecting terms of the same order in τ, we find the two sets of integral equations

$$2\pi\phi_j^0 + \iint_{S_B} \phi_j^0 \frac{\partial G^0}{\partial n} dS = \begin{cases} \iint_{S_B} G^0 n_j dS, & j = 1,\ldots,6 \\ 4\pi\phi_0, & j = D \end{cases} \tag{36}$$

$$2\pi\phi_j^1 + \iint_{S_B} \phi_j^1 \frac{\partial G^0}{\partial n} dS = 2i\iint_{S_F} \phi_j^0 (\nabla_1 G^0 \cdot \nabla_1\chi + \frac{1}{2} G^0 \nabla_1^2 \chi) dS$$
$$- \iint_{S_B} \phi_j^0 \frac{\partial G^1}{\partial n} dS + \begin{cases} \iint_{S_B} \left(G^1 - \frac{1}{i\nu}\nabla G^0 \cdot \nabla\chi_s\right) n_j dS, & j = 1,\ldots,6 \\ 0, & j = D \end{cases} \tag{37}$$

where $j = D$ means the diffraction problem. The zero on the right hand side of the diffraction problem stems from the fact that the incident-wave potential ϕ_0 is independent of τ. We note that the left hand sides of eqs. (36)-(37) involve exactly identical operators. The mathematical and numerical difference between the two equations are thus the right hand sides. The integral equations are solved by a conventional panel method, with the singularities of the Green function integrated analytically.

6 The first-order forces

6.1 Added mass and damping

The radiation force and moment is obtained from the Bernoulli equation as

$$F_i = \text{Re}\ \left(-i\sigma\xi_j e^{i\sigma t} f_{ij}\right) \tag{38}$$

where $i, j = 1, \ldots, 6$. The complex force coefficients f_{ij} are defined as

$$f_{ij} \equiv i\sigma a_{ij} + b_{ij} = \rho \iint_{S_B} (i\sigma\phi_j + U\nabla\chi_s \cdot \nabla\phi_j) n_i dS \tag{39}$$

where a_{ij} are the added mass coefficients and b_{ij} the damping coefficients. It is shown by Wu and Eatock-Taylor (1990) and by Nossen, Grue and Palm (1991) that the Timman-Newman relations, $f_{ij}(U) = f_{ji}(-U)$, are valid for a body of general shape, provided that the forward speed is small. This result is a generalization of Timman and Newman (1962) where a steady disturbance field χ is neglected, with no restrictions, however, that the forward speed should be small. An immediate consequence of the Timman-Newman relations is that

$$f_{ii}(\tau) = f_{ii}(0) + o(\tau) \tag{40}$$

Thus, to leading order the diagonal added mass and damping coefficients only depend on the current speed through the frequency of encounter. The generalized Timman-Newman relations are confirmed by numerical computations.

6.2 The exciting forces

The diffraction force and moment is given as

$$F_i = \Re[-\rho e^{i\sigma t} \iint_{S_B} (i\sigma\phi + U\nabla\chi_s \cdot \nabla\phi) n_i dS] \equiv \Re(Ae^{i\sigma t} X_i) \tag{41}$$

where $i = 1, \ldots, 6$, and ϕ is the total diffraction potential, given by (7) with $\xi_j = 0, j = 1, \ldots 6$. In Nossen, Grue and Palm (1991) generalized Haskind relations valid for small forward speed are derived. These express the exciting forces in terms of the incident wave-potential ϕ_0 and the reversed-flow radiation potentials $\psi_j, j = 1, \ldots 6$ so that the first order exciting forces can be computed without knowing the scattering potential ϕ_7. The result reads

$$X_i = \rho g \sqrt{\frac{2\pi}{K}} \frac{\nu}{K} H_i^-(\beta + \pi + 2\tau \sin\beta) e^{i\pi/4} + o(\tau) \tag{42}$$

where H_i^- denotes the amplitude distribution of the ith reversed flow potential, and is obtained from H_i by replacing τ by $-\tau$ (but keeping ν). H_i is found by introducing (16) in (29), which gives

$$\begin{aligned} H_i(\theta) = &-\frac{1}{4\pi} \iint_{S_B} \left(\phi_i \frac{\partial h}{\partial n} - (h - \frac{\tau}{i\nu} \nabla\chi_s \cdot \nabla h) n_j\right) dS \\ &+ \frac{1}{2\pi} i\tau \iint_{S_F} \phi_i (\nabla_1 h \cdot \nabla_1 \chi + \frac{1}{2} h \nabla_1^2 \chi) dS \end{aligned} \tag{43}$$

The amplitude $h(\xi, \theta)$ of the Green function is given by (26).

7 The mean horizontal drift force and the mean yaw moment

The mean drift force and yaw moment may be computed by direct pressure integration or by using the far-field method. The latter, which is obtained by applying the momentum equation, is most accurate and will be applied here. The mean drift force $\boldsymbol{F}$ is then given by

$$\boldsymbol{F} = -\overline{\iint_{S_\infty} (p\boldsymbol{n} + \rho \boldsymbol{v}\boldsymbol{v} \cdot \boldsymbol{n}) dS} \tag{44}$$

and the yaw moment M_z by

$$M_z = -\boldsymbol{k} \cdot \overline{\iint_{S_\infty} (p\boldsymbol{r} \times \boldsymbol{n} + \rho \boldsymbol{r} \times \boldsymbol{v}\boldsymbol{v} \cdot \boldsymbol{n}) dS} \tag{45}$$

where an overbar denotes time-average. Introducing the velocity potential, we obtain for the x-component of $\boldsymbol{F}$, i.e. in the current direction

$$\begin{aligned} F_x = \rho \int_0^{2\pi} -\frac{1}{2g}\left[\overline{\left(\frac{\partial \Phi}{\partial t}\right)^2} - U^2 \overline{\left(\frac{\partial \Phi}{\partial x}\right)^2}\right]_{z=0} \cos\theta R d\theta \\ +\rho \int_0^{2\pi} \int_{-\infty}^0 \left[\frac{1}{2}\overline{|\nabla \Phi|^2} \cos\theta - \overline{\frac{\partial \Phi}{\partial x}\frac{\partial \Phi}{\partial R}}\right] dz R d\theta \end{aligned} \tag{46}$$

and for the y-component, i.e. orthogonal to the current direction

$$\begin{aligned} F_y = \rho \int_0^{2\pi} -\frac{1}{2g}\left[\overline{\left(\frac{\partial \Phi}{\partial t}\right)^2} - U^2 \overline{\left(\frac{\partial \Phi}{\partial x}\right)^2}\right]_{z=0} \sin\theta R d\theta \\ +\rho \int_0^{2\pi} \int_{-\infty}^0 \left[\frac{1}{2}\overline{|\nabla \Phi|^2} \sin\theta - \overline{\frac{\partial \Phi}{\partial y}\frac{\partial \Phi}{\partial R}}\right] dz R d\theta \\ +\rho U \int_0^{2\pi} \frac{1}{g}\left[\overline{\frac{\partial \Phi}{\partial \theta}\left(\frac{\partial \Phi}{\partial t} - U\frac{\partial \Phi}{\partial x}\right)}\right]_{z=0} d\theta \end{aligned} \tag{47}$$

The contribution to the moment from the first order velocities and to the leading order in U is given by

$$M_z = -\rho \int_0^{2\pi} \int_{-\infty}^0 \overline{\frac{1}{R}\frac{\partial \Phi'}{\partial \theta}\frac{\partial \Phi'}{\partial R}} R dz d\theta + \frac{\rho U}{g} \int_0^{2\pi} \overline{\frac{\partial \Phi'}{\partial t}(y\frac{\partial \Phi'}{\partial R} - x\frac{1}{R}\frac{\partial \Phi'}{\partial \theta})} R d\theta \tag{48}$$

where $\Phi' = \Phi + Ux$. Let us then insert

$$\Phi = \Re e^{i\sigma t} A \frac{ig}{\omega}(\phi_0 + \phi_B) - Ux \tag{49}$$

where ϕ_0 is given by

$$\phi_0 = e^{Kz - iK(x\cos\beta + y\sin\beta)} \tag{50}$$

and ϕ_B is given by

$$\phi_B = R^{-1/2} H(\theta) e^{k_1(\theta)(z - iR\sqrt{1 - 4\tau^2 \sin^2\theta})} + O(\frac{1}{R}) \qquad \text{as } R \to \infty \tag{51}$$

$H(\theta)$ is related to $H_i(\theta), i = 1, ...7$ by

$$H(\theta) = H_7(\theta) + \frac{\sigma\omega}{g} \sum_{j=1}^{6} \frac{\xi_j}{A} H_j(\theta) \tag{52}$$

where $H_j(\theta), j = 1, ...6$ is given by (43), and $H_7(\theta)$ is given by

$$H_7(\theta) = -\frac{1}{4\pi}\left\{\int\int_{S_B} \phi_D \frac{\partial h}{\partial n} dS - 2i\tau \int\int_{S_F} \phi_D(\nabla_1 h \cdot \nabla_1 \chi + \frac{1}{2} h \nabla_1^2 \chi) dS\right\} \quad (53)$$

Averaging with respect to time, and applying the method of stationary phase, we obtain for F_x and F_y

$$\frac{F_x}{\rho g A^2} = -\frac{\nu}{4K}\left\{\int_0^{2\pi} (\cos\theta + 2\tau \sin^2\theta)|H(\theta)|^2 d\theta + 2\cos\beta \Re(S)\right\} + o(\tau) \quad (54)$$

$$\frac{F_y}{\rho g A^2} = -\frac{\nu}{4K}\left\{\int_0^{2\pi} (\sin\theta - 2\tau \sin\theta\cos\theta)|H(\theta)|^2 d\theta + 2\sin\beta \Re(S)\right\} + o(\tau) \quad (55)$$

where

$$S = \sqrt{\frac{2\pi}{\nu}} e^{i\pi/4} H^*(\beta + 2\tau\sin\beta) \quad (56)$$

A star denotes complex conjugate. For the yaw moment we obtain

$$\frac{M_z}{\rho g A^2} = -\frac{1}{4K}\Im\{\int_0^{2\pi} (1 - 2\tau\cos\theta) H \frac{dH^*}{d\theta} d\theta\}$$
$$-\frac{1}{2K}\Im\{\frac{\nu}{K} S' + \tau\sin\beta S\} + o(\tau) \quad (57)$$

where S is given by (56) and S' is given by

$$S' = \sqrt{\frac{2\pi}{\nu}} e^{i\pi/4} (H'(\beta + 2\tau\sin\beta))^* \quad (58)$$

Here H' denotes derivative with respect to θ. It should be noted that to the same order there are also contributions to the mean yaw moment from second order velocities which are not known by linearized theory.

8 Numerical results and discussion

Let us then study the mean drift force and the mean yaw moment in an example where the model is a turret production ship being $L = 230m$ long, $B = 41m$ broad and with the bow heading along the positive x-axis. We apply no moorings in the example, i.e. the ship is freely floating. The half of the ship is discretized with 380 panels which corresponds to an average panel size of $\sim 12m^2$. For small Froude number $U/\sqrt{gB}$ we expand the drift force and yaw moment by

$$F_x = F_{x0} + Fr \times \frac{\partial F_x}{\partial Fr} \quad (59)$$

$$F_y = F_{y0} + Fr \times \frac{\partial F_y}{\partial Fr} \quad (60)$$

$$M_z = M_{z0} + Fr \times \frac{\partial M_z}{\partial Fr} \quad (61)$$

where the subscript "0" denotes the value at zero forward speed. We show numerical results for wave frequencies between $\omega = 0.35s^{-1}$ and $\omega = 0.85s^{-1}$ which corresponds to an incoming wave length λ between $503m$ and $85m$. For smaller values of ω than $0.35s^{-1}$

the forces are vanishing. For $\omega \simeq 0.95s^{-1}$, which corresponds to an incoming wave length of $\lambda = 68m$, the solution by the panel method becomes irregular and cannot be used. We therefore stop the computations at $\omega = 0.85s^{-1}$. As a control of the computations we evaluate the energy flux at control volume far away from the body. Since there are no dissipative forces in the model, the energy flux vanishes, which is confirmed within a good accuracy in the computations.

Let us first discuss the x-component of the mean drift force, i.e. the component along the forward speed direction, which is displayed in figure 1 for waves with incidence angle $\beta = 160^o$ and 180^o (head waves) and in figure 2 for incidence angle $\beta = 140^o$. The figures show that we obtain almost the the same values of F_x and $\partial F_x/\partial Fr$ for incidence angle β between 160^o and 200^o. Even an incidence angle of $\beta = 140^o$ gives, practically speaking the same values of F_x and $\partial F_x/\partial Fr$ as for head waves. We remark that F_x and $\partial F_x/\partial Fr$ always have the same sign, with the magnitude of the latter being 5-10 times larger than F_x at zero forward speed. This means that a forward speed $U = 2ms^{-1}$ of the ship, i.e. a Froude number $Fr = U/\sqrt{gB} \simeq 0.1$, will increase the value of the mean drift force by 50-100% in the present example. Correspondingly, if $U = -2ms^{-1}$, $F_x \simeq 0$. In figure 3 we have displayed values of F_y and $\partial F_y/\partial Fr$ for incoming waves with $\beta = 160^o$, and in figure 4 for $\beta = 140^o$. Not surprisingly, we observe that $\partial F_y/\partial Fr$ is small compared to the value of F_y, which means that the lateral component of the mean horizontal drift force is very little influenced by a small forward speed in this example. The same conclusion does not, however, apply for the values of the mean yaw moment about the z-axis, which we have displayed in figures 5 and 6. The figures show that the value of M_z increases with a small increment in the forward speed. In fact, the value of $\partial M_z/\partial Fr$ is almost exactly ten times the value of M_{z0} when the angle of incidence is 140^o. We thus conclude that a forward speed of $U = 2ms^{-1}$ leads to a doubling of the zero speed values of F_x and M_z, while F_y remains unchanged. Correspondingly, a speed $U = -2ms^{-1}$ backwards reduces F_x and M_z practically speaking to zero.

In the examples above we observe that a small speed against the incoming waves is increasing the value of the drift force component along the speed direction. This may not, however, always be true. It was found by Nossen, Grue and Palm (1991) that the wave drift damping for complex bodies may become negative. This is illustrated in figure 7 which shows the mean drift force F_{x0} and $\partial F_x/\partial Fr$ for a platform which is composed by four vertical cylinders, each of radius a, draft $3a$ and mounted to a ring-like pontoon with breadth $2a$, height $1.4a$ and an outer diameter of $11.8a$. The cylinder centers are forming a square of sides $7a$. Keeping in mind that the wave drift damping for one single cylinder is positive, we ascribe the negative values of $\partial F_x/\partial Fr$ to wave interaction which takes place due to the four cylinders. Negative value of $\partial F_x/\partial Fr$ is leading to negative damping which may destabilize the motions of the body.

It is of interest to estimate the wave drift damping for the ship due to irregular waves and compare with drag damping due to skin friction which is the other dominant damping force for length-wise motions of the ship. The wave drift damping due to an irregular sea with power spectrum denoted by $S(\omega)$ reads

$$D_{WD} = Fr \times 2\int_0^\infty S(\omega)d\omega \frac{\partial F_x/A^2}{\partial Fr} \tag{62}$$

Let us introduce the significant wave height H_s of the irregular sea which is defined by

$$2\int_0^\infty S(\omega)d\omega = \frac{1}{8}H_s^2 \tag{63}$$

In the case when $\partial F_x/\partial Fr$ has a small variation with ω, we may approximate D_{WD} by

$$D_{WD} \simeq \frac{Fr}{8} H_s^2 \frac{\partial F_x/A^2}{\partial Fr} \tag{64}$$

The skin friction drag D_F is given by

$$D_F = \frac{1}{2} C_F \rho U^2 S_B \tag{65}$$

where S_B denotes the area of the wetted hull. Let us assume that $U = 1ms^{-1}$. The Reynolds number is then $O(10^8)$ which gives that the skin friction coefficient is $C_F \simeq 2 \times 10^{-3}$ (see Newman 1977, p.31). The Froude number is $U/\sqrt{gB} = 0.05$. We thus have

$$\frac{D_{WD}}{D_F} = \frac{H_s^2}{B^2} \frac{\partial F_x/\rho g A^2 B}{\partial Fr} \times 10^2 \tag{66}$$

Assuming that $H_s = 4m$, which corresponds to a peak frequency $\omega = 0.63s^{-1}$ of the Pierson-Moskowitz spectrum, we have $H_s/B \simeq 0.1$. Furthermore, from figures 1 and 2 we obtain $\frac{\partial F_x/\rho g A^2 B}{\partial Fr} \simeq 2$, and we conclude that

$$\frac{D_{WD}}{D_F} \simeq 8 \tag{67}$$

which means that the wave drift damping totally dominates the friction drag.

Drag due to separated flow is for the platform completely dominating the skin friction. The drag force D reads

$$D = \frac{1}{2} C_D \rho U^2 S \tag{68}$$

where S denotes the vertical cross-sectional area of the four vertical columns and the ring-pontoon of the platform, which may be approximated by $S \sim 44a^2$ (a the radius of the columns). The value of the drag coefficient for Reynolds number of the order 10^7 is approximately $C_D \sim 0.6$. For the platform we thus have

$$\frac{D_{WD}}{D} = \frac{1}{100Fr} \frac{H_s^2}{a^2} \frac{\partial F_x/\rho g A^2 a}{\partial Fr} \tag{69}$$

(where $Fr = U/\sqrt{ga}$). Let the radius of the columns be $a = 15m$ and the significant wave height be $H_s = 6m$, which corresponds to a peak frequency of the Pierson-Moskowitz spectrum determined by $\omega^2 a/g \simeq 0.4$. From figure 7 we then have $\frac{\partial F_x/\rho g A^2 a}{\partial Fr} \simeq 7$, which gives

$$\frac{D_{WD}}{D} \simeq \frac{0.011}{Fr} \tag{70}$$

This means that the wave drift damping is larger than the drag damping when $U < 0.13ms^{-1}$ in this case.

9 Acknowledgements

Financial support for this work has been granted by the Royal Norwegian Council for Science and the Humanities (NAVF) and by Saga Petroleum A/S. The WAMIT radiation/diffraction program has been provided by Veritas Sesam Systems A/S. The body discretizations and most of the forward speed code are due to Dr. Jan Nossen.

References

[1] GRUE, J. AND PALM, E., Currents and wave forces on ships and marine structures, in Dynamics of marine vehicles and structures in waves. Proc. IUTAM Symposium, Brunel University, Uxbridge, UK, 1990, Ed. W. G. Price, Elsevier 1991.

[2] HUIJSMANS, R.H.M. AND HERMANS, A.J., A fast algorithm for computation of 3-D ship motions at moderate forward speed. *4th International Confer. on Numerical Ship Hydrodynamics*, 1985.

[3] NEWMAN, J.N., Marine Hydrodynamics. The MIT Press, Cambridge, MA 1977.

[4] NEWMAN, J.N., The theory of ship motions. *Advances in Applied Mechanics* **18**, 1978, 221-280.

[5] NOSSEN, J., GRUE, J. AND PALM, E., Wave forces on three-dimensional floating bodies with small forward speed. J. Fluid Mech 1991 (to appear).

[6] OGILVIE, T.F. AND TUCK, E.O., A rational strip theory of ship motions: part 1. Report No 013,The Department of Naval Architecture and Marine Engineering, The University of Michigan, College of Engineering, 1969.

[7] TIMMAN, R. AND NEWMAN, J.N., The coupled damping coefficients of a symmetric ship. *J. of Ship Res.* **5**, 1962, 1-7.

[8] WICHERS, J.E.W. AND SLUIJS, M.F., The influence of waves on the low frequency hydrodynamic coefficients of moored vessels. *Proc. Offshore Technology Conference, Houston, OTC 3625*, 1979.

[9] WICHERS, J.E.W. AND HUIJSMANS, R.H.M., On the low frequency hydrodynamic damping forces acting on offshore moored vessels. *Proc. Offshore Technology Conference, Houston, OTC 4831*, 1984.

[10] WU, G. X. AND EATOCK-TAYLOR, R. The hydrodynamic force on an oscillating ship with low forward speed. *J. Fluid Mech*, **211**, 1990, 333-353.

[11] ZHAO, R., FALTINSEN, O.M., KROKSTAD, J.R. AND AANESLAND, V., Wave-current Interaction Effects on Large-Volume Structures. *Proc. of the International Confer. on the Behaviour of Offshore Structures*, 1988.

[12] ZHAO, R. AND FALTINSEN, O.M., Interaction between current, waves and marine structures. *5th International Confer. on Numerical Ship Hydrodynamics*.1989.

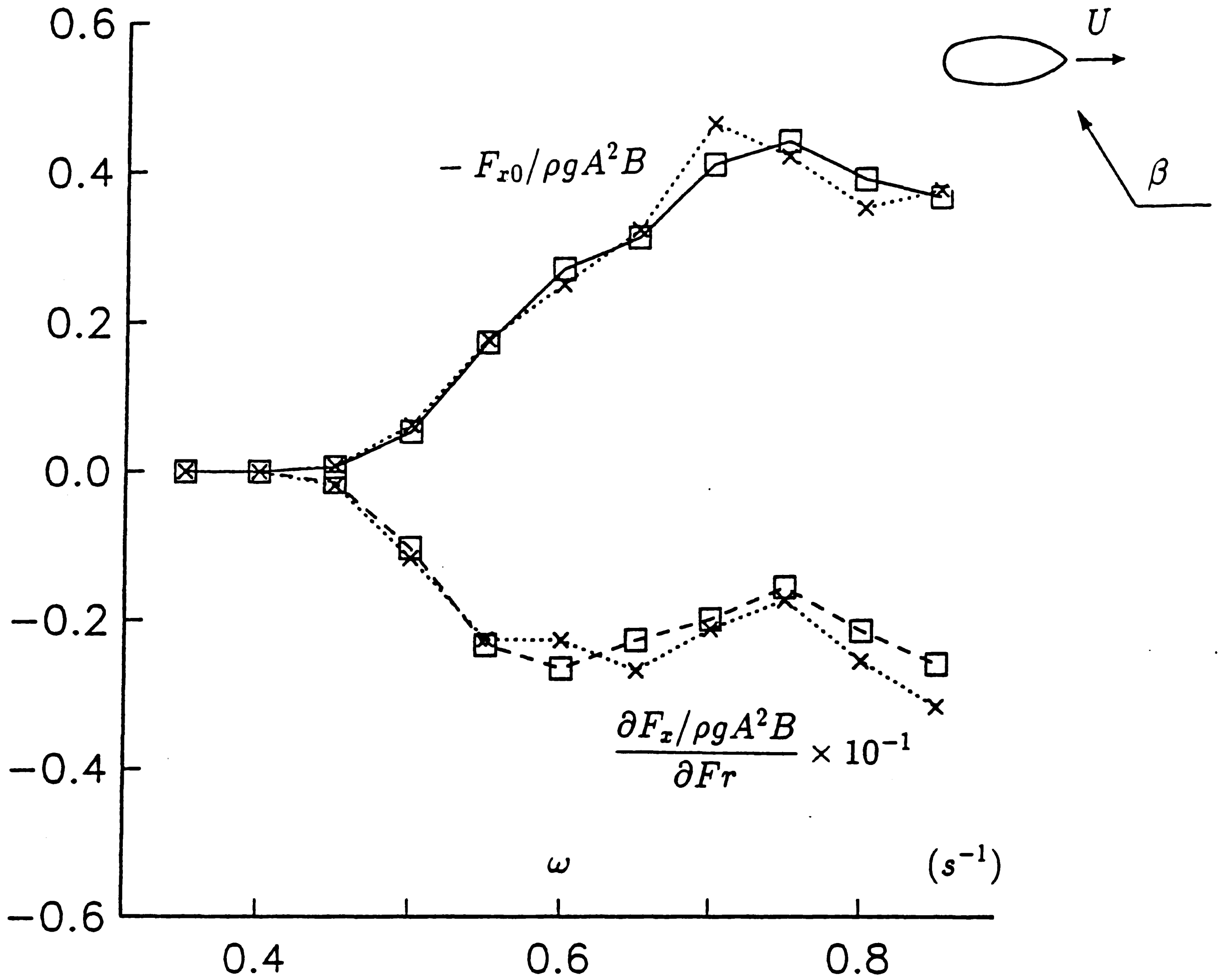

Figure 1: Mean drift force F_{x0} at zero forward speed (solid line) and wave drift damping coefficient $\partial F_x/\partial Fr$ (dashed line) vs. wave frequency ω of the incoming waves. Incidence angle $\beta = 160^o$. Dotted lines: F_{x0} and $\partial F_x/\partial Fr$ for $\beta = 180^o$ (head waves). $\partial F_x/\partial Fr$ is obtained by numerical differentiation of F_x computed for $Fr = \pm 0.02$.

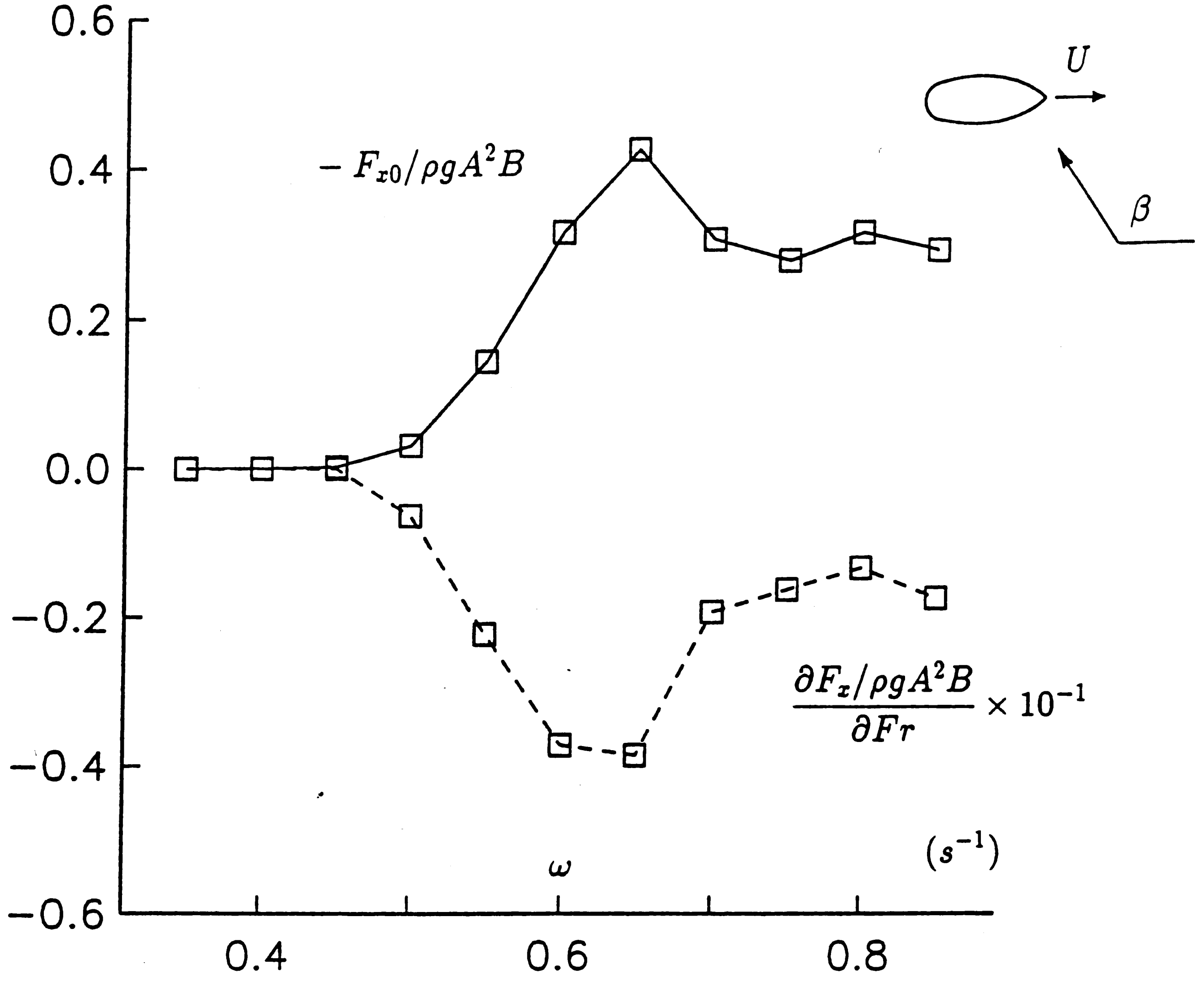

Figure 2: Same as figure 1 but $\beta = 140°$.

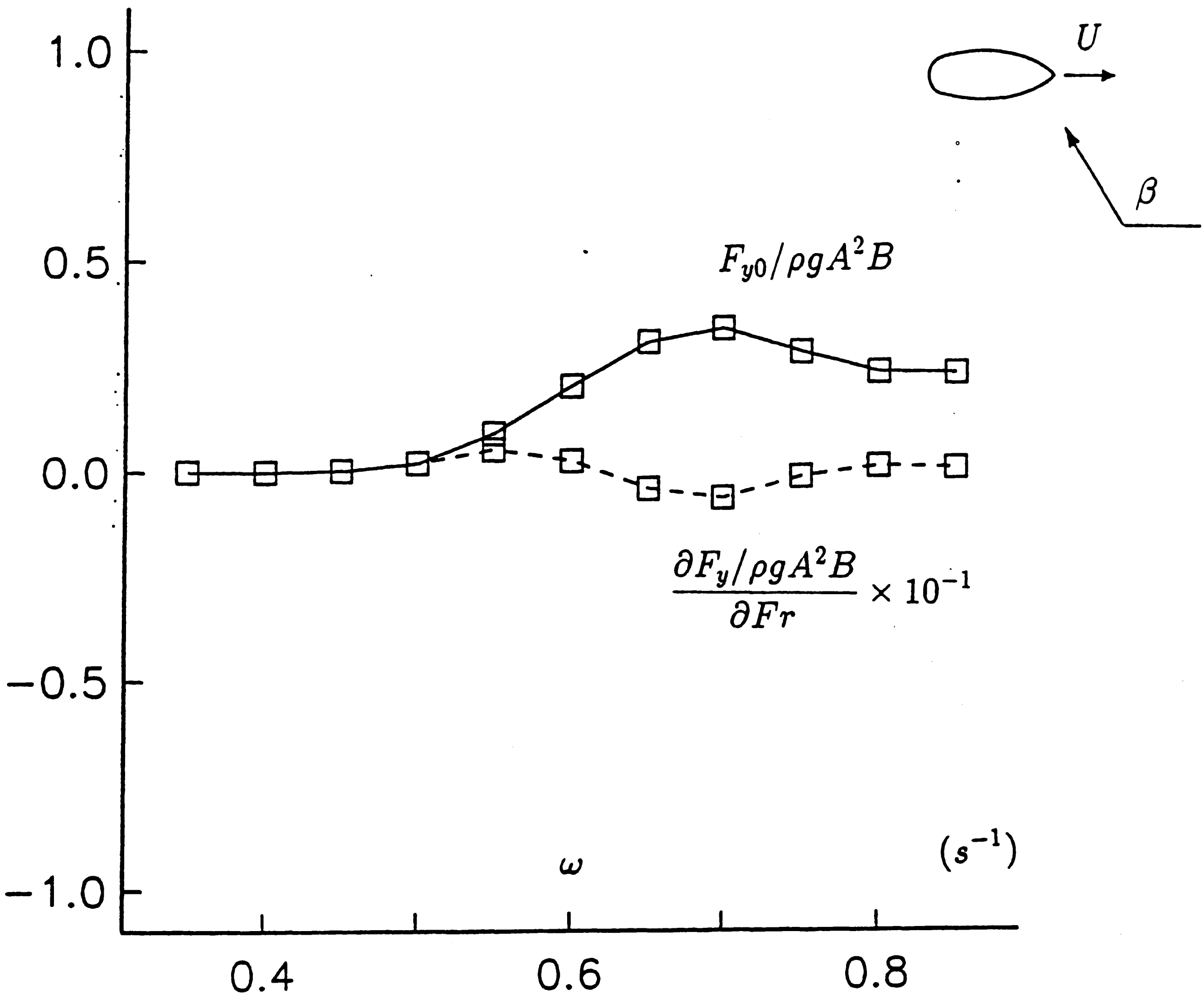

Figure 3: Lateral component of the mean drift force F_{y0} at zero forward speed (solid line) and $\partial F_y/\partial Fr$ (dashed line) vs. wave frequency ω of the incoming waves. Incidence angle $\beta = 160°$. $\partial F_y/\partial Fr$ is obtained by numerical differentiation of F_y computed for $Fr = \pm 0.02$.

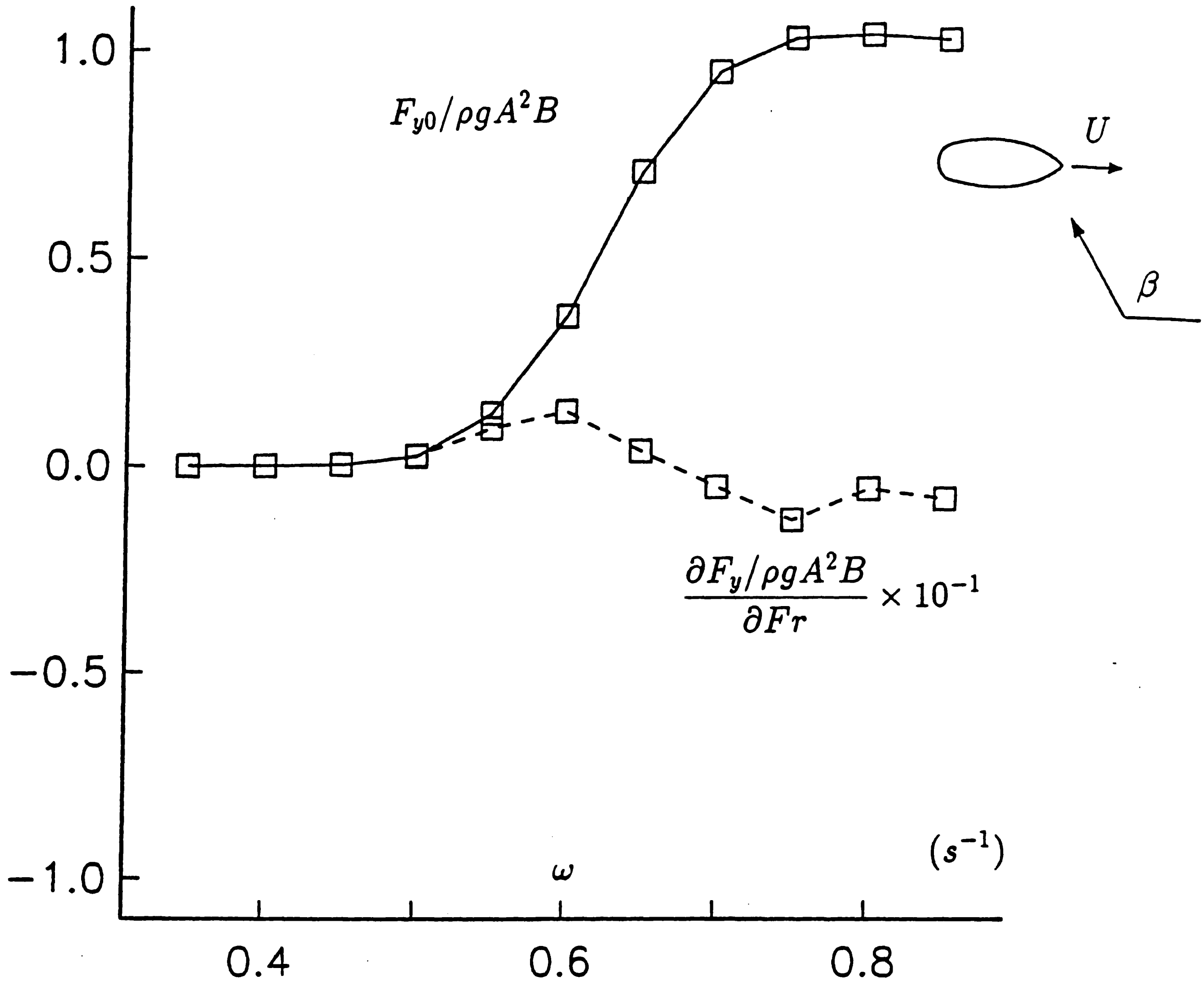

Figure 4: Same as figure 3 but $\beta = 140^o$.

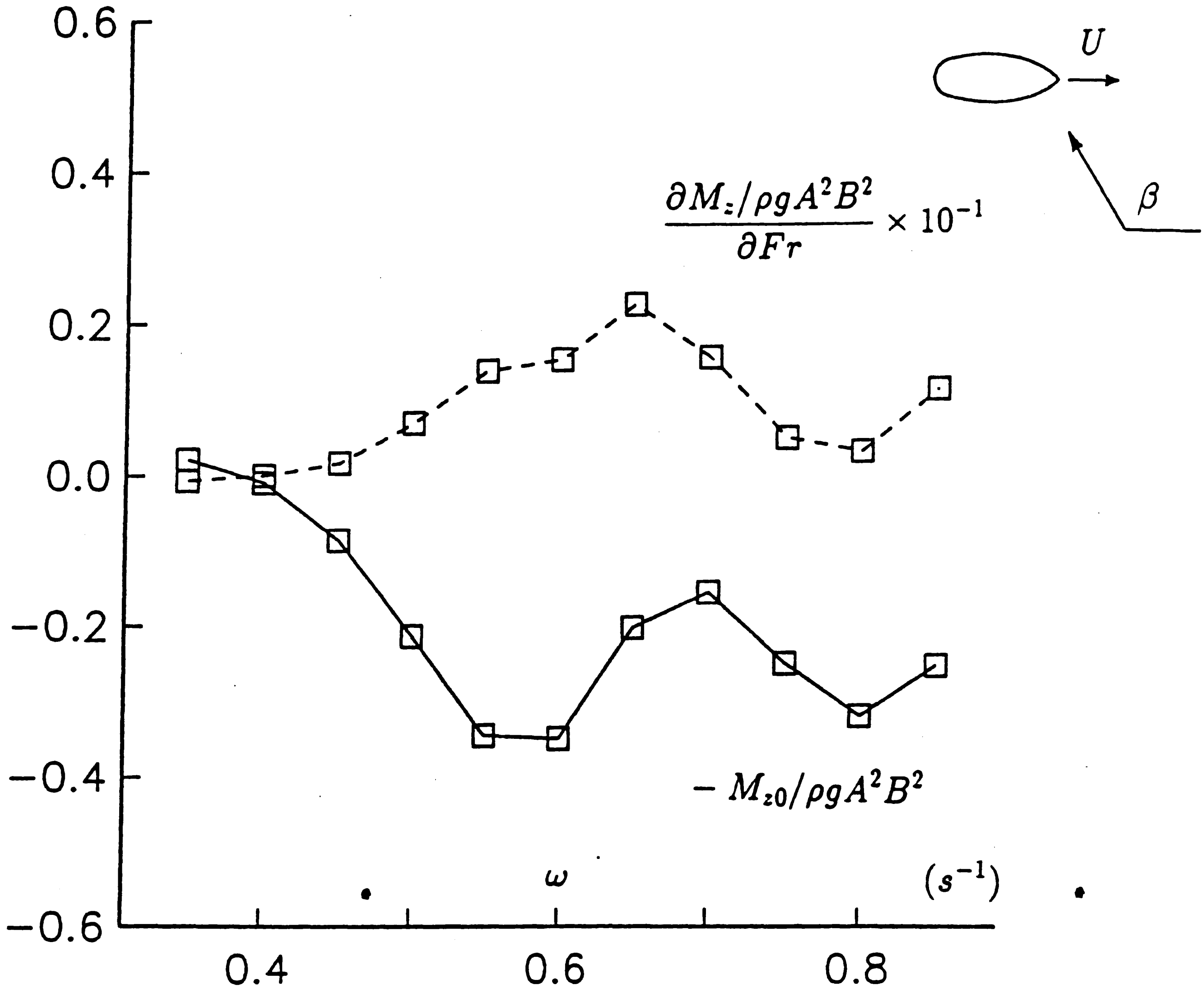

Figure 5: Mean yaw moment M_{z0} at zero forward speed (solid line) and $\partial M_z/\partial Fr$ (dashed line) vs. wave frequency ω of the incoming waves. Incidence angle $\beta = 160^o$. $\partial M_z/\partial Fr$ is obtained by numerical differentiation of M_z computed for $Fr = \pm 0.02$.

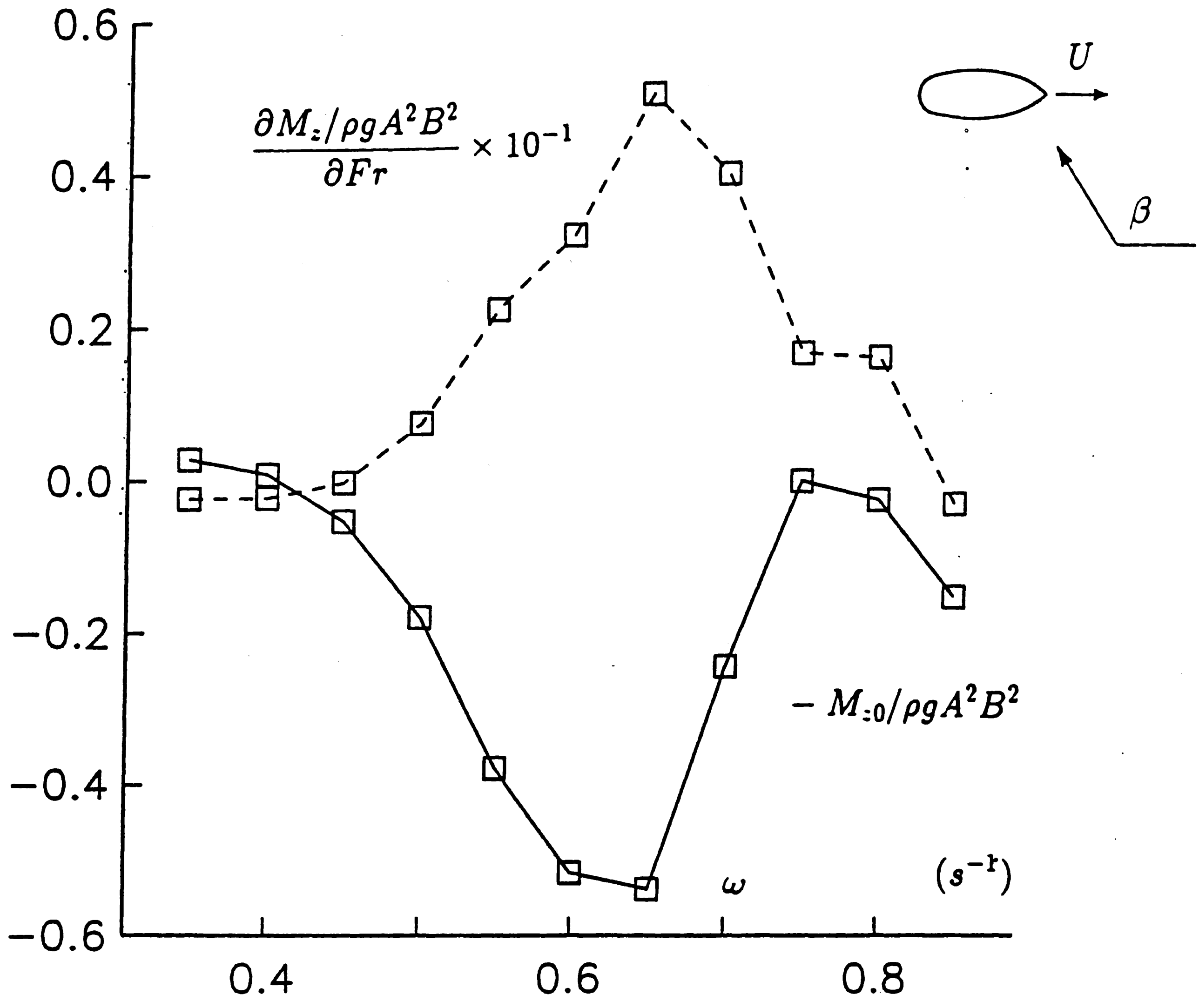

Figure 6: Same as figure 5 but $\beta = 140^{\circ}$.

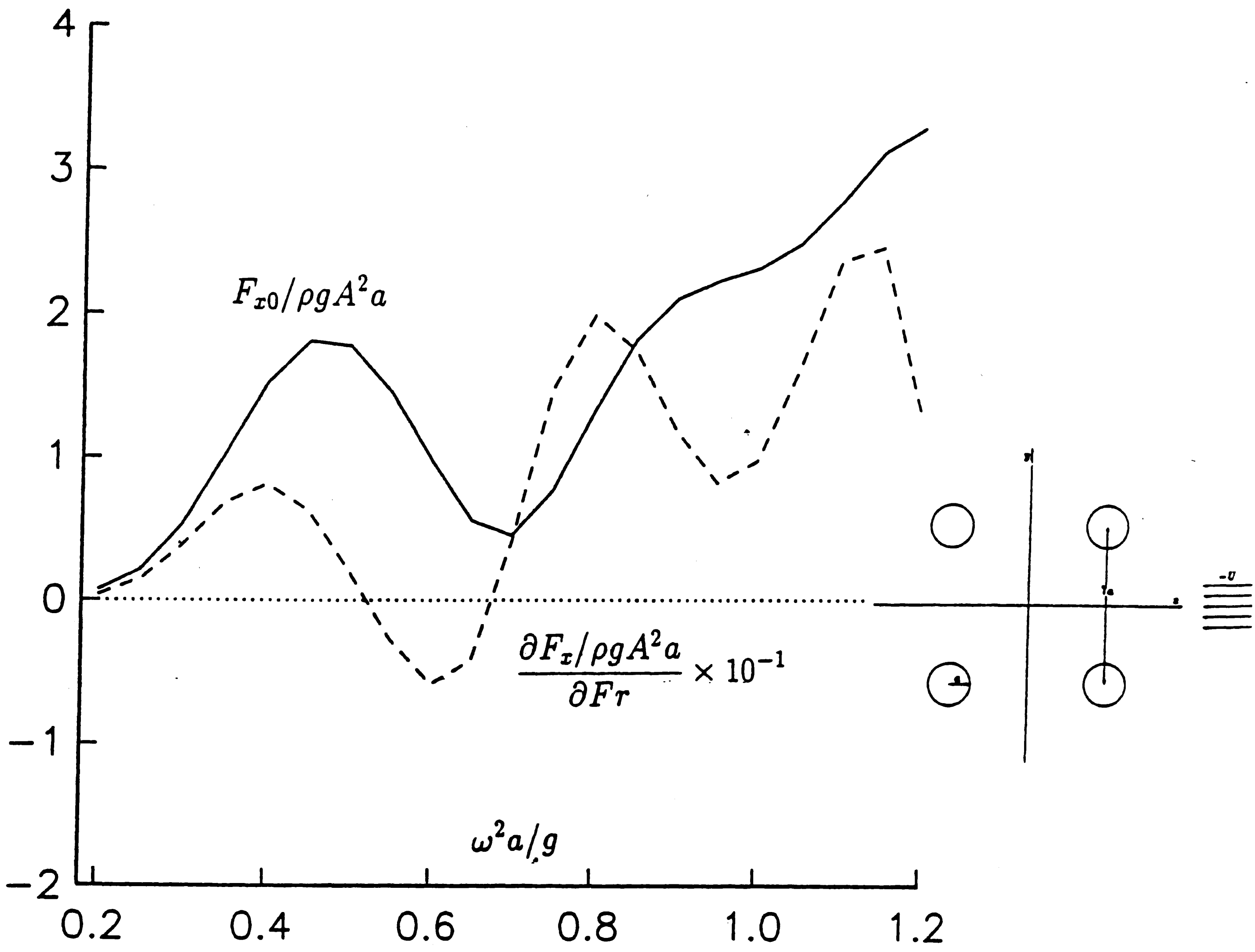

Figure 7: Mean drift force F_{x0} (solid line) and wave drift damping coefficient $\partial F_x/\partial Fr$ (dashed line) for an offshore platform vs. wave number of the incoming waves. Incoming head waves. Platform free to surge in linear motions. $\partial F_x/\partial Fr$ is obtained by numerical differentiation of F_x computed for $Fr = \pm 0.005$. (Nossen, Grue and Palm 1991).